Multimedia Tools and Applications (2020) 79:2127–2159
https://doi.org/10.1007/s11042-019-08225-5

A blind video watermarking algorithm robust to lossy video compression attacks based on generalized Newton complex map and contourlet transform

Milad Jafari Barani[1] · **Peyman Ayubi**[2] · **Milad Yousefi Valandar**[1] · **Behzad Yosefnezhad Irani**[2]

Received: 7 October 2018 / Revised: 26 July 2019 / Accepted: 13 September 2019 /
Published online: 15 November 2019

Abstract

The rapid growth of fast communication networks for digital video transmission has created a need to copyright protection for these media. Digital video can be manipulated easily by users with various motivations. Compression is the most common attack that users can apply on videos in order to eliminate digital video copyright. Proposed technique in this article is specially designed for resisting against compression attacks. This method is presented a blind and robust watermarking method to copyright protection in digital video. In the proposed method, the coefficients of the contourlet transform are extracted and then encrypted watermark embedded into video with using the singular value decomposition (SVD). Embedding watermark in SVD domain increases the robustness of proposed method against attacks. In the embedding process and watermark encryption, pseudo-random numbers generated by the proposed new chaotic map, which is a generalized two-dimensional complex map based on the Newton model. The PSNR, SSIM, BER, and NCC measures examine the performance of the proposed method in terms of robustness and visual quality.

Keywords Video watermarking · Newton complex map · Contourlet transform · Singular value decomposition

✉ Milad Jafari Barani
milad.jafare@gmail.com

Peyman Ayubi
p.ayubi@iaurmia.ac.ir

Milad Yousefi Valandar
milad_yousefi@hotmail.com

Behzad Yosefnezhad Irani
b.yousefnezhad@iaurmia.ac.ir

[1] Young Researchers and Elite Club, Urmia Branch, Islamic Azad University, Urmia, Iran

[2] Department of Computer Engineering, Urmia Branch, Islamic Azad University, Urmia, Iran

1 Introduction

Digital media surrounded human life. People now use digital media in their lifestyle, education, entertainment and work. Every person in his life is certainly confronting with digital media at his home, work, or even on driving. One of the reasons maybe is the expansion of strong communication networks such as the internet. This communication platform provides a huge amount of information for users anywhere in the world. The huge part of this information is digital videos and images, which are undeniable on human life [44].

News agencies, entertainment and film making companies, as well as social networks all use video as the main part of their resources. The widespread using of this media in the presentation of concepts and information are inherent to its nature, which can be interpreted and understood easily by human mind [19, 31, 48]. Generally, video is referred to the visual information that is captured by a camera, and it is sequentially framed. The increasing development of computer industry and growing the power of hardware processing system alongside with many benefits have caused problems for producers of digital media, including video [53]. In the general view, the most important weakness of digital media is the ability of changing their content, due to the existence of powerful software and computer systems. Various data hidding methods have been proposed to prevent this vulnerability [14, 45, 56–58]. Watermarking is one of the main branches of data hiding science, and it can maintain the integrity and authenticity of the media by embedding the logo or watermark into digital content [43].

Digital watermarking is a set of techniques that aimed to maintain the integrity of digital media by embedding desired content into the cover media [22, 49, 51]. These techniques can be divided into three general categories based on resistance to attacks: 1- robust algorithms, 2- fragile algorithms, and 3- semi-fragile algorithms. The robust watermarking algorithms are capable to maintain the embedded content against attacks [8, 23, 37, 46]. Fragile algorithms do not have any resistance against attacks, and most of them are used to media authentication and tamper detection of digital media [16, 61]. Semi-fragile algorithms are robust against certain attacks, such as image compression or signal processing attacks such as digital media quality improvement, which are fragile against most attacks [36]. The application of robust algorithms is in the field of copyright protection in digital media [12, 33, 34]. This feature is an important concept for commercial and scientific applications. Usually, there are various attacks on videos that could endanger the embedded content and eliminate the owner's copyright [32].

Some sort of attacks which perform on digital media are deliberately or caused by some communication channel's problems. For example, noises are attacks that caused by communication lines, recording system faults, and so on. There are also attacks that aim to improve the quality of digital works, such as the various filters that apply to the media. However, the most important attacks that could threaten the integrity and authenticity of digital works are compression attacks and format changing, which are very common in video files [7]. Compression is a process which a typical user can easily change format and the size of video files by using different compression software in computer or mobile phone. Therefor in practical applications, the most important attack on the video files is compression. We will continue to review the papers in the digital watermarking area in the following.

An efficent technique based on Dual-tree complex wavelet transform is proposed for robust video watermarking [5]. In this method, resistance of watermarking algorithm has increased against geometric distortions. The proposed algorithm embedded the watermark

in the U element of YUV domain. In [41] a watermarking method is proposed to protect the copyright of digital video. In this technique, the 3D wavelet transform is used and the embedding algorithm is performed using the spread spectrum. In order to increase the robustness of the video watermarking against rotation and collusion attacks an efficient technique is presented in [28]. The proposed method is blind and based on a discrete cosine transform, and the embedding algorithm is performed on the luminance channel.

A new secure watermarking algorithm based on SVD proposed in [42]. This approach is a robust technique and embedding process done in contourlet transform domain. Hybrid watermarking method proposed based o DWT and SVD in [4]. Proposed algorithm is robust method which can resist against some sort of image processing attacks. In [3], based on SVD and artificial bee colony a multipurpose watermarking algorithm is proposed. A new robust watermarking method based on SVD proposed in [64]. This algorithm utilize PCA and complex wavelet transform. In [54] a new semi blind video watermarking algorithm proposed based on SVD and DWT. In [15] an algorithm for watermark embedding and digital media content protection is presented. In this scheme, the watermark is divided into separate parts and embeds in various video shot. This technique is transform base and uses Motion Activity Analysis (MAA). Watermarking algorithm for standard MPEG-2 video's based on fast SVD is proposed [60]. This technique in embedding process utilizes discrete cosine transform (DCT) and singular value decomposition (SVD). The main advantage of this algorithm is resistance against compression and simple geometric attacks.

A blind watermarking technique for H.264 compressed video has been suggested in [39]. In this algorithm syntactic elements of video have been used. In [6] a new robust technique for video watermarking based on blocking techniques is proposed. For increased robustness, the speed-up robust feature (SURF) has been used. Radon transform for video watermarking has been used in [35]. The 1-D discrete Fourier transform has been used for Watermarking. The most important advantage of this method is its simplicity and practicality. Chaotic video encryption has been used in [23]. The proposed scheme is based on secure key-frame and embeds watermark as robust. In this approach, SVD has been used for embedding in discrete wavelet transform domain. A video watermarking technique with combination of various transforms proposed in [1]. This method has good imperceptibility and robustness. In this technique, Arnold's transform has been used to scrambling the twenty-four sections of cover image. Multi-resolution wavelet analysis has been used for video watermarking in [46]. This approach for protecting copyrights of videos contents embeds the watermark in the selected coefficients from the Y channel of each frame. The efficiency of the algorithm has improved using error correction codes.

In order to increase robustness against camcorder-based copy attacks, video watermarking approach is proposed in [20]. In this technique, the Scale Invariant Feature Transform (SIFT) is used to find geometric invariant features of the video. In this algorithm, the three-dimensional wavelet transform has been used. A watermarking technique based on pseudo-3D discrete cosine transform has been proposed in [24], which is based on quantization index modulation (QIM) and resistant to image processing attacks. The embedding process done in the DCT transform domain. This approach does not have proper robustness against geometric attacks such as scaling and rotation.

By reviewing the various papers in the video watermarking domain, we can see that the most articles have been used to investigate the power of proposed algorithms for attacks such as rotation, crop, etc. In practice, these attacks are not common attacks but instead, the most common types of attacks or manipulations that may be deliberate or unintentional by ordinary users on videos are compression attacks to reduce the size of the video or to

change the format for display on different devices. Therefore, the most important attacks on digital videos can be compression and format changing. In this paper, evaluation done on variety of compression formats to test the robustness of the proposed method. We also used HD videos because of widespread use in today's media exchanges. In this paper, a new robust watermarking technique has been proposed in the contourlet transform (CT) domain. In the proposed technique, the video frames are initially split into R, G and B color channels. Then, the contourlet transform is applied to each channel, and the sub-bands coefficient of each color channel are extracted. Sub-band selection in the proposed algorithm is performed by generalized two-dimensional Newton complex map. After selecting the sub-bands and the desired block, SVD is applied to that block and the encrypted watermark embedded into the U matrix and watermarked frame generated by the inverse of SVD and contourlet transform. The proposed algorithm has been able to obtain high quality in the embedding algorithm by using contourlet transform and Newton complex map. Also, the use of a sequential embedding mechanism in video frames cause to reduce error rate in extracted watermarks which resulting in a very small error in the final extraction watermark.

The rest of the paper is organized as follows: In the second section, the proposed complex map and generalized version of Newton's model is explained. In the third part, definition of Singular value decomposition is displayed. Section four proposes video watermarking algorithm in two separated parts that include embedding and extraction process. Experimental results are presented in section five. Finally, the last section deals with the conclusions of the paper.

2 Chaos and fractal

Dynamical system is a well-known system that used in many different sciences like mathematics and physics. This system has completely unpredictable behaviors that seem they are random, but they have deterministic properties. Generally, the behaviors of dynamical systems are defined by simple equations that they are called chaotic maps [21]. Sensitivities to initial conditions and control parameters are the main features of these maps that caused they have been used in many security systems, economics, city planning, etc. Sometimes the results of chaotic maps can be repeated in the different scales, and created a strange attractor with same structure. The graphical presentation of these results showed an interesting figure. If we zoom on the figure, we see the smaller copies of the larger structure. As a matter of fact, these self similar structures called fractals. Mandelbrot set, Newton's fractal and Julia set are the most well-known fractals that have been created many interesting images [26]. Next sub section explains the Newton's fractal and the proposed chaotic map.

2.1 Newton complex map

The classic Newton fractal [25] has two parameters that z_0 is initial parameters and α is control parameter. This fractal generates different bounded sets to create interesting shapes. Generally, this fractal cannot be used as a pseudo number generator (PRNG) because the generated numbers in this fractal converge to $+\infty$ and $-\infty$ after several iterations. This situation is not a suitable feature of the PRNGs [38]. However, in PRNGs, the folding feature balanced the values of generated sequence and the chaotic oscillation is produced by stretching feature. In the main structure of classic newton complex map there is no folding

process in order to control the map and output value always is a single number. In order to solve this problem, the proposed model uses a complex folding procedure to generate more than one number in the generating process. Moreover, this procedure returns the generated number to the interval [0 1].

2.1.1 Proposed two dimensional Newton map

Color images or video frames are multi-dimensional data because they use the Red, Green and Blue channels. In this paper, in order to select three dimensional image blocks a new two dimensional chaotic map is proposed. The following equations represent the proposed polynomial functions of Newton's complex map:

$$\begin{cases} f_1(Z_1) = Sin(Z_1), \\ f_2(Z_2) = Sin(Z_2). \end{cases} \tag{1}$$

Now, with using these equations, two dimensional model is proposed as follows:

$$\begin{cases} Z_1^{n+1} = Z_1^n - \alpha \times \frac{f_1(Z_1^n) \times f_2(Z_2^n)}{f_1'(Z_1^n)}, \\ Z_2^{n+1} = Z_2^n - \beta \times \frac{f_2(Z_2^n) \times f_1(Z_1^n)}{f_2'(Z_2^n)}. \end{cases} \tag{2}$$

In the proposed model in order to control the interval between [0, 1] , Complex Folding (CFold) function utilized. This is a new heuristic function which proposed as following:

$$\begin{cases} Z_1^{n+1} = [Z_1^n - \alpha \times \frac{\sin(Z_1^n) \times \sin(Z_2^n)}{\cos(Z_1^n)}] \quad CFold \quad 1, \\ Z_2^{n+1} = [Z_2^n - \beta \times \frac{\sin(Z_2^n) \times \sin(Z_1^n)}{\cos(Z_2^n)}] \quad CFold \quad 1. \end{cases} \tag{3}$$

The CFold in (3) is calculated as following:

$$Z \quad CFold \quad 1 = (Z^{Real} \quad mod \quad 1) + (Z^{Imag} \quad mod \quad 1) \times 1i. \tag{4}$$

Note that in (4), $Z_1^{Real}, Z_2^{Real}, Z_1^{Imag}, Z_2^{Imag} \in [0, 1]$ and $\alpha, \beta \in [1, 4]$. Graphical representation of generalization process displays in Fig. 1.

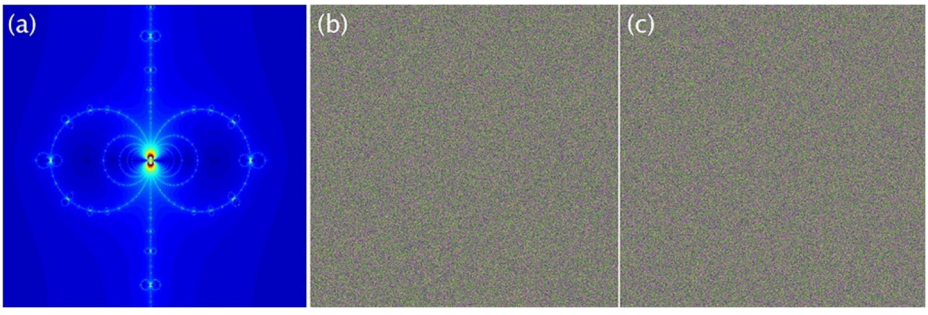

Fig. 1 Generalization proposed map based on classic Newton map. **a** Classic Newton complex map **b** Proposed map generated space for Z_1^{Real} **c** Proposed map generated space for Z_2^{Real}

Algorithm 1 Embedding process of proposed method.

input : Video, Newton complex map keys: α, β, $Z_1 \& Z_2$, Watermark (W)
output: Watermarked video frame.

$Frame$ = selected video frame ;
$R = Frame(:,:,1)$; $G = Frame(:,:,2)$; $B = Frame(:,:,3)$;
$[LowPass_R, HighPass_R]$ = Contourlet Transform (R);
$[LowPass_G, HighPass_G]$ = Contourlet Transform (G);
$[LowPass_B, HighPass_B]$ = Contourlet Transform (B);
$LL(:,:,1)=[LowPass_R]$;
$LL(:,:,2)=[LowPass_G]$;
$LL(:,:,3)=[LowPass_B]$;
$[w_x, w_y]$= sizeof (Watermark) ;
$[ll_x, ll_y]$= sizeof (LL);
Mask=zeros($\frac{ll_x}{4}, \frac{ll_y}{4}, 3$);
for i = *1 to* w_x **do**
  for j = *1 to* w_y **do**
    while *1* **do**
      $z_1^{n+1} = z_1^n - \alpha \times \frac{\sin(z_2^n)\sin(z_1^n)}{\cos(z_1^n)}$;
      $z_2^{n+1} = z_2^n - \beta \times \frac{\sin(z_1^n)\sin(z_2^n)}{\cos(z_2^n)}$;
      $x = \lfloor Real(z_1^{n+1}) \times 10^{14} \rfloor \; Mod \; \frac{ll_x}{4}$;
      $y = \lfloor Imag(z_1^{n+1}) \times 10^{14} \rfloor \; Mod \; \frac{ll_y}{4}$;
      $ch = \lfloor Real(z_2^{n+1}) \times 10^{14} \rfloor \; Mod \; 3$;
      if $Mask([x][y][ch]) == 0$ **then**
        break while ;
    $EK = z_2^{Imag} > 0.5$;
    $W(i,j) = W(i,j) \oplus EK$;
    $B = LL[x \times 4 + 1 \; to \; x \times 4 + 4][y \times 4 + 1 \; to \; y \times 4 + 4][ch]$;
    $[u, s, v] = SVD(B)$;
    $avg = average(|u([1][1])|, |u([2][1])|)$;
    if $W([i][j]) == 0$ **then**
      $Temp = ||u([1][1])| - |u([2][1])||$;
      if $|u([1][1])| > |u([2][1])| \; \&\& \; Temp < T$ **then**
        $u([1][1]) = sign(u([1][1])) \times (avg + \frac{T}{2})$;
        $u([2][1]) = sign(u([2][1])) \times (avg - \frac{T}{2})$;
    if $W([i][j]) == 1$ **then**
      $Temp = ||u([2][1])| - |u([1][1])||$;
      if $|u([1][1])| < |u([2][1])| \; \&\& \; Temp > T$ **then**
        $u([1][1]) = sign(u([1][1])) \times (avg - \frac{T}{2})$;
        $u([2][1]) = sign(u([3][1])) \times (avg + \frac{T}{2})$;
    $B = u \times s \times v^T$;
    $LL[x \times 4 + 1 \; to \; x \times 4 + 4][y \times 4 + 1 \; to \; y \times 4 + 4][ch] = B$;
    $Mask([x][y][ch]) = 1$
$[LowPass_R] = LL(:,:,1)$;
$[LowPass_G] = LL(:,:,2)$;
$[LowPass_B] = LL(:,:,3)$;
R = Inverse Contourlet Transform $([LowPass_R, HighPass_R])$;
G = Inverse Contourlet Transform $([LowPass_G, HighPass_G])$;
B = Inverse Contourlet Transform $([LowPass_B, HighPass_B])$;
$Frame(:,:,1) = R$; $Frame(:,:,2) = G$; $Frame(:,:,3) = B$;
Keep the final z_1, z_2 for using as the initial conditions of next frame;
Return Embedded Frame ;

2.2 Bifurcation diagram and Lyapunov exponent

Bifurcation diagram is a useful method to show the sensitivity of the proposed map in changing the control parameters. This diagram shows the chaotic behaviors of maps in the best numerical interval. Lyapunov exponent is the other well-known method to show the fixed points, periodic orbits and chaotic attractor in proposed map. In this method, if $\lambda > 0$, the generated numbers of proposed method are chaotic, if $\lambda = 0$, the generated numbers are fixed-point, and if $\lambda < 0$, the generated numbers are periodic. To calculate the Lyapunov exponent of proposed map following equations are used. Note that in this equation $N = 10000$.

$$\begin{cases} \lambda_1(Z_1^{Real} + \delta_0) = \frac{1}{N}\Sigma_{n=1}^{N} \log(|\frac{f^n(Z_1^{Real}+\delta_0)-f^n(Z_1^{Real})}{\delta_0}|) \\ \lambda_2(Z_1^{Imag} + \delta_0) = \frac{1}{N}\Sigma_{n=1}^{N} \log(|\frac{f^n(Z_1^{Imag}+\delta_0)-f^n(Z_1^{Imag})}{\delta_0}|) \\ \lambda_3(Z_2^{Real} + \delta_0) = \frac{1}{N}\Sigma_{n=1}^{N} \log(|\frac{f^n(Z_2^{Real}+\delta_0)-f^n(Z_2^{Real})}{\delta_0}|) \\ \lambda_4(Z_2^{Imag} + \delta_0) = \frac{1}{N}\Sigma_{n=1}^{N} \log(|\frac{f^n(Z_2^{Imag}+\delta_0)-f^n(Z_2^{Imag})}{\delta_0}|) \end{cases} \tag{5}$$

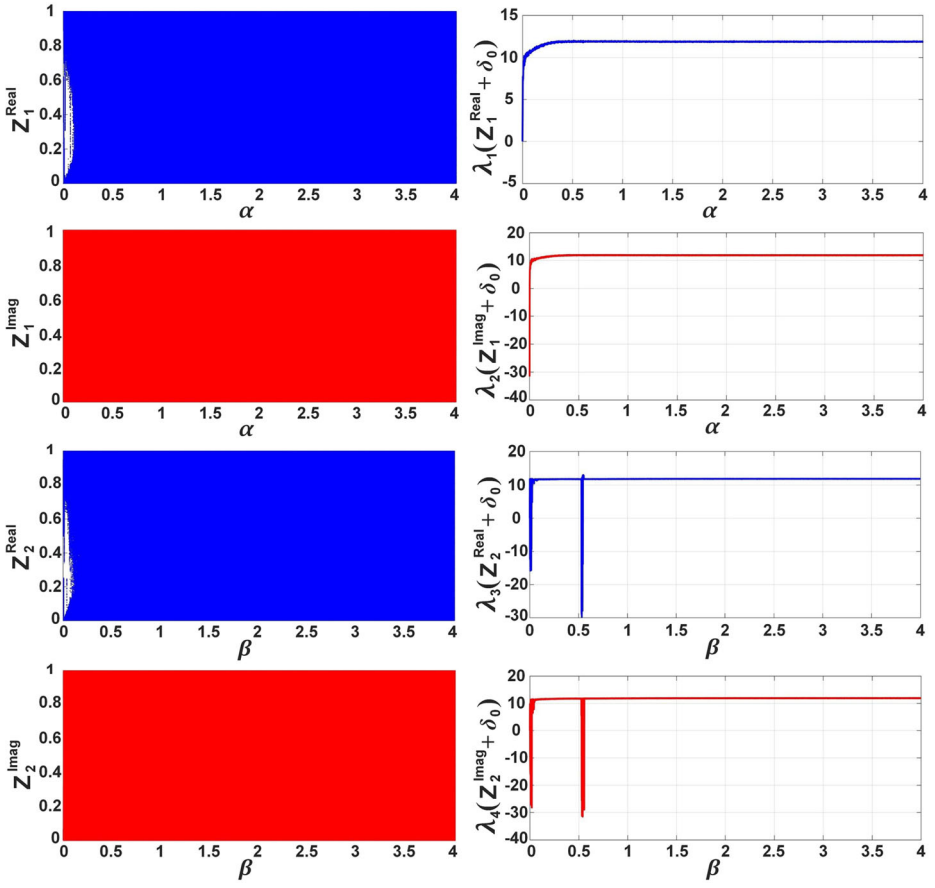

Fig. 2 Bifurcation and Lyapunov exponent of proposed complex map for: **a** Z_1^{Real}, α, **b** Z_1^{Imag}, α, **c** Z_2^{Real}, β, **d** Z_2^{Imag}, β

Figure 2 displays the bifurcation diagrams of proposed map and the chaotic intervals for each control key. Also in this figure the bifurcation diagrams of Z_1^{real}, Z_2^{real}, Z_1^{imag} and Z_2^{imag} for different values of α and β illustrated. Proposed Complex map has six key include $[Z_1^{Real}, Z_2^{Real}, Z_1^{Imag}, Z_2^{Imag}] \in [0, 1]$ and $\alpha, \beta \in [1, 4]$ and has long term security and 2^{280} key length. This key space is large enough to resist brute-force attack. To show the randomness of the proposed map, the NIST statistical test is used. Table 1 displays the output results of the proposed map for NIST test. The results of ENT and DIEHARD test suite also displayed in Tables 2 and 3 respectively.

3 Singular value decomposition

One of the most important tools in the modern numerical analysis is singular value decomposition (SVD). In 1870, Beltrami and Jordan proposed SVD for square matrices [29], and this technique was generalized by Autonne on rectangular matrices. In general, the SVD theory is expressed as follows: Let $A \in \mathbb{R}_r^{m\times n}[\mathbb{C}_r^{m\times n}]$. Then exist orthogonal matrices $U \in \mathbb{R}^{m\times m}[\mathbb{C}^{m\times m}]$ and $V \in \mathbb{R}^{n\times n}[\mathbb{C}^{n\times n}]$ which:

$$A = U \sum V^T [U \sum V^H] \tag{6}$$

Where

$$\sum = \begin{pmatrix} S & 0 \\ 0 & 0 \end{pmatrix} \tag{7}$$

and $S = diag(\sigma_1, ..., \sigma_r)$ with $\sigma_1 \geq ... \geq \sigma_r > 0$. $\sigma_1, ..., \sigma_r$ with $\sigma_{r+1} = 0, ..., \sigma_n = 0$ are single values of the A matrix, which is the positive square roots of the eigenvalues of

Table 1 The results of NIST test suite for generated sequence with proposed chaotic map

Test name	Z_1^{real}	Z_2^{real}	Z_1^{imag}	Z_2^{imag}
Frequency	0.9269	0.6898	0.6881	0.8081
Block-Frequency	0.9178	0.6676	0.6463	0.6920
Cumulative-Sums (Forward)	0.8574	0.6905	0.7181	0.7952
Cumulative-Sums (Reverse)	0.7510	0.7738	0.7270	0.8493
Runs	0.9245	0.7239	0.7692	0.8714
Longest-Runs	0.8128	0.9693	0.8028	0.7577
Rank	0.7398	0.7716	0.6335	0.6435
FFT	0.9756	0.6733	0.7044	0.9952
Non-Overlapping-Templates	0.8197	0.9919	0.6109	0.9540
Overlapping-Templates	0.6825	0.7026	0.7950	0.6388
Universal	0.7199	0.7630	0.8311	0.7042
Approximate Entropy	0.7880	0.8376	0.6943	0.7336
Random-Excursions	0.6916	0.7043	0.7831	0.8716
Random-Excursions Variant	0.9376	0.8408	0.9852	0.6539
Serial 1	0.7076	0.8603	0.5462	0.6791
Serial 2	0.6276	0.6087	0.9305	0.8415
Linear Complexity	0.7246	0.8225	0.8858	0.6305

Table 2 The results of ENT test suite for generated sequence with proposed chaotic map

Test name	Z_1^{real}	Z_2^{real}	Z_1^{imag}	Z_2^{imag}
Entropy	7.999998	7.999992	7.999995	7.999997
Chi-square	239.82	243.31	261.03	252.54
Arithmetic mean	127.9731	127.9425	127.8741	127.9085
Monte Carlo	3.141496	3.141529	3.141528	3.141575
Serial correlation	0.000247	0.000863	0.000371	0.000593

$A^T A$ $[A^H A]$. In mentioned equation U is called left singular vector of A and V is called right singular vector of A.

Singular value decomposition has unique characteristics in the watermarking filed. For example, U matrix has the main coefficients in SVD, which has a high robustness against image processing and geometric attacks. Embeding watermark inside the U matrix will has the least effect on the overall structure of cover video and increase the imperceptibility and robustness of the watermarking algorithm [17]. Hence in the proposed algorithm, the SVD technique is used to embed the watermark into U matrix to make the distribution of the embed values more robust and more invisible.

Table 3 The results of DIEHARD test suite for generated sequence with proposed chaotic map

Test name	Z_1^{real}	Z_2^{real}	Z_1^{imag}	Z_2^{imag}
Birthday spacing	0.5861	0.7312	0.7089	0.6549
Overlapping permutation	0.6761	0.6267	0.6178	0.6215
Binary rank 32×32	0.6901	0.7753	0.6814	0.7883
Binary rank 6×8	0.5523	0.6369	0.8171	0.5347
Bitstream	0.6138	0.5503	0.5221	0.8032
OPSO	0.9341	0.9129	0.6449	0.8175
OQSO	0.9330	0.4971	0.8389	0.7536
DNA	0.9654	0.7038	0.9593	0.6825
Count ones str	0.8665	0.8434	0.7575	0.8214
Count ones byt	0.6379	0.8104	0.6261	0.5057
Parking Lot	0.4868	0.6961	0.7951	0.4704
2DS spheres	0.6467	0.5475	0.5686	0.8984
3DS spheres	0.7153	0.7342	0.9560	0.8257
Squeeze	0.8658	0.9839	0.8811	0.9083
Sums	0.7723	0.8176	0.5985	0.5107
Runs (up)	0.5722	0.5609	0.9055	0.8695
Runs (down)	0.7389	0.5098	0.9264	0.6499
Craps for no. of wins	0.6916	0.8027	0.9128	0.4894
Craps for throws/game	0.7495	0.5496	0.8268	0.4873
Tsang gcd	0.6279	0.6775	0.7251	0.6815
Sts monobit	0.8472	0.7427	0.6109	0.7253
Sts runs	0.5602	0.8541	0.7984	0.6549
Sts serial 1	0.9196	0.8966	0.7835	0.8607
Sts serial 2	0.6712	0.5378	0.6840	0.7848

4 Proposed method

Video watermarking is one of the most important techniques to copyright protection. In this paper, for digital video watermarking, a robust and blind algorithm is proposed that is a free-format technique. The embedding and extraction processes in proposed method are based on contourlet transform (CT). The proposed algorithm utilizes RGB color channels and SVD, which improves the visual quality of the proposed algorithm. Also in order to improve the security of embedding and extraction algorithms, a new complex map based on Newton's model is used. In the proposed algorithm, watermark is also encrypted by new complex map for security improvement. In the extraction process of the proposed algorithm, a new technique is used to examine the correlation to correct the quality of extracted watermark. In the following, the embedding and extraction algorithms are separately explained.

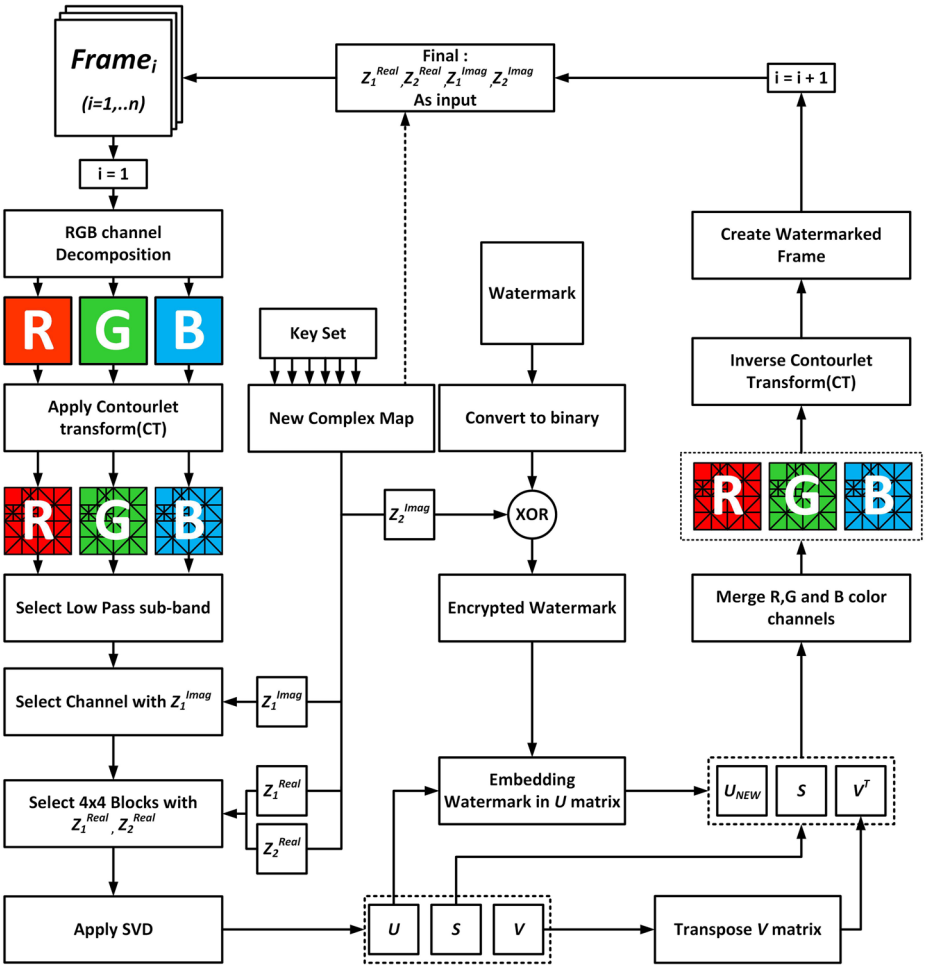

Fig. 3 Embedding algorithm block diagram of proposed algorithm

4.1 Watermarking embedding

The proposed watermarking algorithm starts with the embedding process in each frame and Fig. 3 displays this process. In order to embedding watermark bits into digital video following steps are used (Algorithm 1):

Step 1: Input cover video and watermark logo,
Step 2: Initiate Newton complex map with α, β, z_1, z_2,
Step 3: Divide video frame to R,G and B color channels,
Step 4: Apply CT on each video frame in different color channels,
Step 5: Extract CT sub-bands and select LL of each R,G,B channels,
Step 6: Generate Newton Complex map output include z_1^{Real}, z_1^{Imag}, z_2^{Real}, z_2^{Imag} with keyset,
Step 7: Select color channel randomly using with z_1^{Imag},
Step 8: Divide selected sub band to 4×4 blocks and choose one 4×4 block using $z_1^{Real} and z_2^{Real}$,

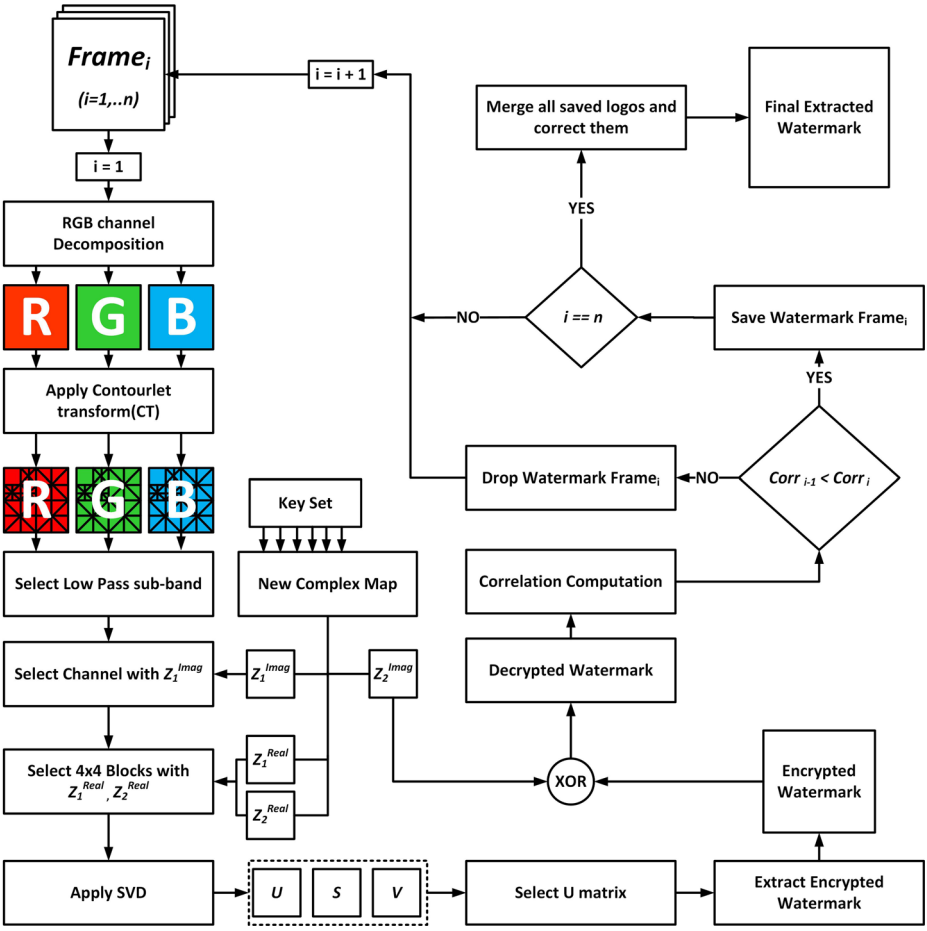

Fig. 4 Extraction algorithm block diagram of proposed algorithm

Step 9: Apply SVD on selected block,
Step 10: Extract U, S, V matrix,
Step 11: Convert Watermark to binary and XOR with z_2^{Imag} in order to generate encrypted sequence,
Step 12: Embedding the encrypted watermark in U matrix and create U_{New},
Step 13: Convert V matrix to V transpose,
Step 14: Merge U_{New}, S and V^T and create the corresponding color channel,
Step 15: Merge R,G,B color channels and apply inverse contourlet transform,
Step 16: Generate watermarked frame and for next frame keep the final z_1, z_2 for using as initial condition of next frame.

Algorithm 2 Extraction process of proposed method.

input : Watermarked video, Newton complex map keys: α, β, $Z_1 \& Z_2$.
output: Watermark.

$Frame$ = selected video frame;
$R = Frame(:,:,1)$; $G = Frame(:,:,2)$; $B = Frame(:,:,3)$;
$[LowPass_R, HighPass_R]$ = Contourlet Transform (R);
$[LowPass_G, HighPass_G]$ = Contourlet Transform (G);
$[LowPass_B, HighPass_B]$ = Contourlet Transform (B);
$LL(:,:,1)$=$[LowPass_R]$;
$LL(:,:,2)$=$[LowPass_G]$;
$LL(:,:,3)$=$[LowPass_B]$;
$[w_x, w_y]$= sizeof (Watermark);
$[ll_x, ll_y]$= sizeof (LL);
Mask=zeros($\frac{ll_x}{4}$, $\frac{ll_y}{4}$, 3);
for i = *1 to* w_x **do**
  for j = *1 to* w_y **do**
    while *1* **do**
      $z_1^{n+1} = z_1^n - \alpha \times \frac{\sin(z_2^n)\sin(z_1^n)}{\cos(z_1^n)}$;
      $z_2^{n+1} = z_2^n - \beta \times \frac{\sin(z_1^n)\sin(z_2^n)}{\cos(z_2^n)}$;
      $x = \lfloor Real(z_1^{n+1}) \times 10^{14} \rfloor \; Mod \; \frac{ll_x}{4}$;
      $y = \lfloor Imag(z_1^{n+1}) \times 10^{14} \rfloor \; Mod \; \frac{ll_y}{4}$;
      $ch = \lfloor Real(z_2^{n+1}) \times 10^{14} \rfloor \; Mod \; 3$;
      if $Mask([x][y][ch]) == 0$ **then**
        break while ;
    $B = LL[x \times 4 + 1 \; to \; x \times 4 + 4][y \times 4 + 1 \; to \; y \times 4 + 4][ch]$;
    $[U, S, V] = SVD(B)$;
    if $|u[1][1]| > |u[2][1]|$ **then**
      $EW(i, j) = 0$;
    else
      $EW(i, j) = 1$;
    $EK = z_2^{Imag} > 0.5$;
    $EW(i, j) = EW(i, j) \oplus EK$;
    $Mask([x][y][ch]) = 1$
Keep the final z_1, z_2 for using as the initial conditions of next frame ;
Return EW (Extracted Watermark) ;

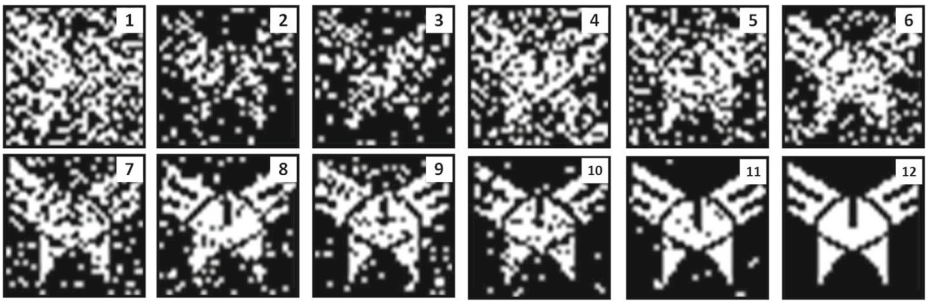

Fig. 5 Correction steps of extracted logo in proposed extraction algorithm

4.2 Extraction algorithm

After embedding the watermark into the video frames, it is time to examine the extraction algorithm. To extract the watermark and verify its functionality, the algorithm first accepts

Fig. 6 Standard High Definition (HD) videos from Xiph.org [18], 1) aspen, 2) blue sky, 3) controlled burn, 4) crowd run, 5) dinner, 6) factory, 7) four people, 8) in to tree, 9) johnny, 10) kristen and sara, 11) life, 12) mobcal, 13) old town cross, 14) park joy, 15) parkrun, 16) pedestrian area, 17) red kayak, 18) riverbed, 19) rush field cuts, 20) rush hour, 21) shields, 22) speed bag, 23) station2, 24) stockholm, 25) sunflower, 26) touchdown pass, 27) tractor, 28) vidyo1, 29) vidyo3, 30) vidyo4

video frames as inputs and divides each frame individually into three color channels. The overall extraction algorithm steps are as following (Fig. 4):

Step 1: Input watermarked video and Newton complex map keys,
Step 2: Select one frame of watermarked video,
Step 3: Divide selected video frame to R,G and B color channels ,
Step 4: Apply CT on each video frame in different color channels and extract LL sub-bands of each color channel ,
Step 5: Generate Newton Complex map output include z_1^{Real}, z_1^{Imag}, z_2^{Real}, z_2^{Imag} with keyset,
Step 6: Select color channel randomly using with z_1^{Imag},
Step 7: Divide selected sub band to 4×4 blocks and choose one 4×4 block using $z_1^{Real} and z_2^{Real}$,
Step 8: Apply SVD on selected block and extract U, S, V matrices,
Step 9: Extract encrypted watermark from U matrix,
Step 10: Watermark decryption done by XOR the encrypted watermark with z_2^{Imag} ,
Step 11: Calculate correlation of frame ,
Step 12: If correlation value of current frame grater than the previous frame, go to step 13 else go to step 14 ,
Step 13: Save extracted watermark and if $Frame_{no} < End_{Frame}$ go to step 1 else merge all saved watermarks and go to step 15 ,
Step 14: Drop watermark of $Frame_i$ and go to step 1,
Step 15: Error correction done(accumulate all true and saved watermarks) and final watermark extract.

After the correction of extracting watermarks, the final watermark is created. Notes that the Algorithm 2 shows more precisely the proposed extracting and correction algorithm. Also Fig. 5 displays the extracted watermark correction steps.

5 Experimental results

Using the contourlet transform, which is one of the best transform in the field of video watermarking, we present the proposed method in the previous section. The proposed technique is a SVD-based method which watermark is embedded into the U matrix to increase the robustness of watermarking algorithm. In this section, in order to investigate the performance and efficiency of proposed method in terms of resistance to attacks and imperceptibility of watermarking a set of test videos are used. These test videos have $1080 \times 1920(1080p)$ and $720 \times 1280(720p)$ size and have Y4M format [18] which displayed in Fig. 6. Test videos to examine the impact of compression attacks first taken to uncompressed AVI format. In this paper a 1024-bit (32×32) binary watermark in the embedding process is used. To implement the algorithm, the MATLAB 2017b software is used in the Windows 10 operating system with the Intel Core-i7 processor and 32 GB RAM. In order to analyze the proposed method, PSNR, SSIM, NC, and BER measures have been investigated for robustness and imperceptibility.

5.1 Visual quality measures

Peak signal-to-noise ratio (PSNR) and structural similarity index (SSIM) are two important measures to show the destruction of videos. This paper uses PSNR to measure the quality

of videos after embedding watermark and measures the similarity between original video and watermarked video with SSIM. Generally, PSNR is defined by following equation.

$$PSNR = 10\log_{10}\left(\frac{MAX_{O_v}^2}{MSE}\right) \tag{8}$$

where MAX_{O_v} is the maximum possible pixel value between the frame of original video and the frame of watermarked video. Mean square error (MSE) is defined by:

$$MSE = \frac{1}{mn}\sum_{i=1}^{m}\sum_{j=1}^{n}[O_v(i,j) - W_v(i,j)]^2 \tag{9}$$

Table 4 The results of PSNR and SSIM results after embedding watermark in videos

Videos	PSNR	SSIM	NCC	BER	FrameNo	Resolution
Aspen	47.29	0.9957	1.0000	0.0000	570	1080p
Blue sky	46.97	0.9966	1.0000	0.0000	217	1080p
Controlled Burn	47.90	0.9957	1.0000	0.0000	570	1080p
Crowd run	48.24	0.9976	1.0000	0.0000	500	1080p
Dinner	52.06	0.9969	1.0000	0.0000	950	1080p
Factory	52.74	0.9974	1.0000	0.0000	1339	1080p
Four People	45.63	0.9937	1.0000	0.0000	600	720p
In to tree	48.48	0.9961	1.0000	0.0000	500	1080p
Johnny	47.43	0.9935	1.0000	0.0000	600	720p
Kristen & Sara	47.14	0.9943	1.0000	0.0000	600	720p
Life	50.65	0.9974	1.0000	0.0000	825	1080p
Mobcal	45.01	0.9941	1.0000	0.0000	504	720p
Old town cross	44.89	0.9926	1.0000	0.0000	500	1080p
Park joy	42.56	0.9970	1.0000	0.0000	500	1080p
Park run	42.26	0.9970	1.0000	0.0000	504	720p
Pedestrian	52.43	0.9977	1.0000	0.0000	375	1080p
Red Kayak	48.59	0.9951	1.0000	0.0000	570	1080p
Riverbed	49.38	0.9973	1.0000	0.0000	250	1080p
Rush Field Cuts	47.23	0.9959	1.0000	0.0000	570	1080p
Rush hour	52.76	0.9978	1.0000	0.0000	500	1080p
Shields	45.76	0.9966	1.0000	0.0000	504	720p
Speed Bag	49.33	0.9930	1.0000	0.0000	570	1080p
Station 2	51.53	0.9972	1.0000	0.0000	313	1080p
Stockholm	44.69	0.9942	1.0000	0.0000	604	720p
Sunflower	51.56	0.9976	1.0000	0.0000	500	1080p
Touch down Pass	49.28	0.9950	1.0000	0.0000	570	1080p
Tractor	49.89	0.9969	1.0000	0.0000	690	1080p
Vidyo 1	46.57	0.9933	1.0000	0.0000	600	720p
Vidyo 3	47.25	0.9929	1.0000	0.0000	600	720p
Vidyo 4	46.24	0.9927	1.0000	0.0000	600	720p
Average	48.08	0.9956	1.0000	0.0000	–	–

where O_v is the frame of original video and W_v is the frame of watermarked video, respectively. The frame size of original video is shown by m and n. The SSIM metric is defined by following equation:

$$SSIM(O_v, W_v) = \frac{(2\mu_x\mu_y + C_1)(2\sigma_{xy} + C_2)}{(\mu_x^2 + \mu_y^2 + C_1)(\sigma_x^2 + \sigma_y^2 + C_2)} \tag{10}$$

where the mean intensity of x and y are σ_x and σ_y. The variance of x and y are σ_x^2 and σ_y^2. The co-variance of x and y is σ_{xy}. The averages of x and y are μ_y and μ_x. Variables C_1 and C_2 are used to stabilize the division with weak denominator. Table 4 illustrates the results of video's qualities and similarities after embedding process. This results quite show that the proposed method passes these measures with acceptable ranges. In order to investigate the scalability of proposed method three different video data set include: Hollywood2 just action samples [40], HMDB51 [30] and FCVID [27] were selected. Overall 300 video(100 video from each data set) were selected for evaluation the visual quality and robustness. Table 5 displays the output results which reflects the ability of proposed method achieve high visual quality and robustness.

5.2 Robustness analysis against lossy video compression

In this paper, to test the robustness of proposed algorithm, different types of lossy compression like MPEG4, MPEG2, DIVX, H.264, etc are selected. Generally, this paper uses FFMPEG software to compress watermarked videos to the most types and the commercial Wondershare Software is used for unsupported types. In order to show the robustness of proposed method, this paper calculates normalized correlation (NC) and bit error rate (BER) between original watermark and extracted watermark after applying lossy compression. Normalized correlation is calculated by:

$$NC(W, EW) = \frac{\sum_{i=1}^{m}\sum_{j=1}^{n} W(i,j)EW(i,j)}{\sum_{i=1}^{m}\sum_{j=1}^{n} W^2(i,j)EW^2(i,j)} \tag{11}$$

Table 5 Visual quality and robustness after embedding watermark in different data sets based on PSNR, SSIM , NCC and BER in proposed method

Data set	Result	PSNR	BER	SSIM	NCC
Hollywood 2 [40]	Min	42.03	0.0000	0.9889	1.0000
	Max	50.32	0.0000	0.9977	1.0000
	Std	0.199	0.000	0.023	0.000
	Average	47.13	0.0000	0.9948	1.0000
HMDB51 [30]	Min	43.35	0.0000	0.9895	1.0000
	Max	50.90	0.0000	0.9918	1.0000
	Std	0.188	0.000	0.104	0.000
	Average	48.14	0.0000	0.9905	1.0000
FCVID [27]	Min	44.18	0.0000	0.9717	1.0000
	Max	51.11	0.0000	0.9983	1.0000
	Std	0.332	0.000	0.251	0.000
	Average	49.59	0.000	0.9962	1.0000

Table 6 NC and BER for extracted watermarks after applying different lossy compression on watermarked videos(Part 1)

Videos	ASF		DIVX		DVD		FLV		GIF		H.264	
	NC	BER	NC	BER	NC	BER	NC	BER	NC	BER	NC	BER
Aspen	1.0000	0.0000	1.0000	0.0000	1.0000	0.0000	0.9918	0.3906	1.0000	0.0000	0.8541	8.3555
Blue sky	0.9961	0.1953	1.0000	0.0000	1.0000	0.1953	0.9849	1.1719	1.0000	0.0000	0.8675	7.3711
Control led Burn	0.9863	0.6836	1.0000	0.0000	0.9874	0.9793	0.9115	4.4922	1.0000	0.0000	0.8392	9.8656
Crowd run	0.9043	4.7852	0.9454	2.8320	0.9827	0.9766	0.9327	3.5156	1.0000	0.0000	0.8448	9.5813
Dinner	1.0000	0.0000	1.0000	0.0000	1.0000	0.0000	1.0000	0.0000	1.0000	0.0000	1.0000	0.0000
Factory	0.9941	0.2930	1.0000	0.0000	0.9857	1.0742	0.9835	0.9748	1.0000	0.0000	0.8628	7.0469
Four People	1.0000	0.0000	1.0000	0.0000	0.9905	0.3906	0.9342	3.5156	1.0000	0.0000	0.9647	2.2461
In to tree	0.9824	0.8789	1.0000	0.0000	1.0000	0.0000	0.9881	1.0742	1.0000	0.0000	0.9118	4.3945
Johnny	1.0000	0.0000	1.0000	0.0000	1.0000	0.0000	0.9805	1.1719	1.0000	0.0000	0.9531	2.6367
Kristen And Sara	1.0000	0.0000	1.0000	0.0000	0.9871	0.9772	0.9222	3.8086	1.0000	0.0000	0.8372	8.6914
Life	0.8984	5.0781	0.9826	1.0742	0.9154	4.5898	0.8268	7.9648	1.0000	0.0000	0.8425	9.3711
Mob cal ter	1.0000	0.0000	1.0000	0.0000	1.0000	0.0000	1.0000	0.0000	1.0000	0.0000	0.9438	2.8320
Old town cross	0.9961	0.1953	1.0000	0.0000	1.0000	0.0000	0.9975	0.4883	1.0000	0.0000	0.9346	3.5156
Park joy	0.9355	3.2227	0.8964	5.2734	0.8847	6.0547	0.8582	6.5977	1.0000	0.0000	0.8824	6.0938
Park run	0.9961	0.1953	1.0000	0.0000	1.0000	0.0000	1.0000	0.0000	1.0000	0.0000	0.9886	0.7813
Pedestrian area	0.9727	1.3672	0.9972	0.4883	0.9643	2.0508	0.8924	5.6641	1.0000	0.0000	0.9175	4.3711
Red Kayak	1.0000	0.0000	1.0000	0.0000	0.9968	0.2930	0.9667	2.1484	1.0000	0.0000	0.8694	7.1289
Riverbed	1.0000	0.0000	0.9783	1.3672	1.0000	0.0000	0.9852	0.9766	1.0000	0.0000	0.8621	6.8359
Rush Field Cuts	0.9688	1.5625	0.9643	2.0508	0.9963	0.6836	0.8308	8.3984	1.0000	0.0000	0.8497	9.9102
Rush hour	0.9941	0.2930	1.0000	0.0000	1.0000	0.0000	0.9441	2.9297	1.0000	0.0000	0.8296	9.9987
Shields ter	0.9902	0.4883	1.0000	0.0000	1.0000	0.0000	0.9965	0.2930	1.0000	0.0000	0.9161	4.2969
Speed Bag	0.9980	0.0977	1.0000	0.0000	1.0000	0.1953	0.9981	0.2930	1.0000	0.0000	0.8386	8.7984
Station 2	0.9922	0.3906	1.0000	0.0000	1.0000	0.0000	0.9875	0.7813	1.0000	0.0000	0.8435	9.7711

Table 6 (continued)

Videos	ASF		DIVX		DVD		FLV		GIF		H.264	
	NC	BER	NC	BER	NC	BER	NC	BER	NC	BER	NC	BER
Stockholm	0.9941	0.2930	1.0000	0.0000	1.0000	0.0000	0.9983	0.2930	1.0000	0.0000	0.9537	2.7344
Sunflower	0.9980	0.0977	1.0000	0.0000	0.9873	0.7813	0.8892	6.0547	1.0000	0.0000	0.8548	8.3711
Touch down Pass	0.9961	0.1953	1.0000	0.0000	1.0000	0.0000	0.9537	2.7344	1.0000	0.0000	0.8198	9.9993
Tractor	0.9941	0.2930	0.9973	0.6836	0.9832	1.1719	0.8766	6.7383	1.0000	0.0000	0.8373	8.8228
Vidyo 1	1.0000	0.0000	1.0000	0.0000	0.9979	0.3906	0.9515	2.3438	1.0000	0.0000	0.9624	1.9531
Vidyo 3	1.0000	0.0000	1.0000	0.0000	1.0000	0.0000	1.0000	0.0000	1.0000	0.0000	0.9741	1.3672
Vidyo 4	1.0000	0.0000	1.0000	0.0000	0.9945	0.3921	0.9639	1.7578	1.0000	0.0000	0.9938	0.4883
Average	0.9863	0.6869	0.9920	0.4590	0.9885	0.7065	0.9515	2.5524	1.0000	0.0000	0.8950	5.9210
Videos	HEVC		MJPEG		MKV		MOV		MPEG4		MPEG1	
	NC	BER	NC	BER	NC	BER	NC	BER	NC	BER	NC	BER
Aspen	0.8747	3.3711	1.0000	0.0000	0.7861	9.9742	0.7196	22.8372	1.0000	0.0000	1.0000	0.0000
Blue sky	0.7927	8.9384	0.9962	0.2851	0.7937	9.5864	0.8206	8.3734	1.0000	0.0000	1.0000	0.0000
Control led Burn	0.7994	9.9648	0.9572	2.7344	0.8427	7.7656	0.8017	9.7656	0.9957	0.6836	0.9967	0.6947
Crowd run	0.8495	6.3711	0.9453	3.2227	0.7588	10.5313	0.7325	13.4911	0.9934	0.5859	0.9683	1.7578
Dinner	1.0000	0.0000	1.0000	0.0000	1.0000	0.0000	1.0000	0.0000	1.0000	0.0000	1.0000	0.0000
Factory	0.8636	5.2871	0.9862	1.0742	0.7989	8.3469	0.7114	23.7469	1.0000	0.0000	1.0000	0.0000
Four People	0.7901	9.2539	0.9738	1.6602	0.9736	1.6602	0.9633	2.2461	1.0000	0.0000	1.0000	0.0000
In to tree	0.7795	9.9414	0.9937	0.4883	0.8917	5.3711	0.9109	4.3945	1.0000	0.0000	0.9967	0.2930
Johnny	0.7824	9.8398	1.0000	0.0000	0.9539	2.4414	0.9658	2.2461	1.0000	0.0000	1.0000	0.0000
Kristen And Sara	0.7968	8.7031	0.9724	1.5535	0.8308	8.6914	0.8372	7.6914	1.0000	0.0000	1.0000	0.0000
Life	0.8985	3.8348	0.8027	10.0586	0.8917	5.4379	0.7914	9.2869	0.8963	5.4688	0.9635	1.8555

Table 6 (continued)

Videos	HEVC		MJPEG		MKV		MOV		MPEG4		MPEG1	
	NC	BER	NC	BER	NC	BER	NC	BER	NC	BER	NC	BER
Mob cal ter	0.8721	4.5820	1.0000	0.0000	0.9425	2.8320	0.9427	2.8320	1.0000	0.0000	1.0000	0.0000
Old town cross	0.8059	6.8047	1.0000	0.0000	0.9249	4.1016	0.9346	3.5156	1.0000	0.0000	1.0000	0.0000
Park joy	0.7958	9.5581	0.7759	11.6211	0.7908	8.0938	0.8805	5.0938	0.8697	7.2266	0.9439	2.9297
Park run	0.8481	5.9688	1.0000	0.0000	0.9873	0.7813	0.9816	0.7813	1.0000	0.0000	1.0000	0.0000
Pedestrian area	0.7957	8.5875	0.9364	3.7109	0.7956	9.3616	0.7954	9.5069	0.9815	1.1719	0.9782	1.4648
Red Kayak	0.8725	6.5625	0.9785	1.3672	0.8928	5.4688	0.8573	7.1289	0.9939	0.4883	1.0000	0.1953
Riverbed	0.7894	9.7813	0.9952	0.3775	0.8409	7.8125	0.8669	6.8359	1.0000	0.0000	1.0000	0.0000
Rush Field Cuts	0.7951	9.3759	0.8471	8.2031	0.8562	5.9102	0.7428	15.9502	0.9872	1.0742	0.9348	3.4180
Rush hour	0.8178	8.5471	0.9929	0.6783	0.7987	9.3708	0.7894	9.9467	1.0000	0.0000	0.9924	0.2930
Shields ter	0.9483	4.2227	0.9958	0.2930	0.9153	4.2969	0.9152	4.2969	1.0000	0.0000	1.0000	0.0000
Speed Bag	0.7812	9.2305	1.0000	0.0000	0.8418	8.2031	0.8502	7.3242	1.0000	0.0000	1.0000	0.0000
Station 2	0.7427	8.7734	0.9946	0.3906	0.8847	6.8716	0.7476	15.8711	1.0000	0.0000	1.0000	0.0000
Stockholm	0.8133	8.7070	1.0000	0.0000	0.9436	2.8320	0.9469	2.8320	1.0000	0.0000	1.0000	0.0000
Sunflower	0.7904	7.3711	0.9384	3.4180	0.7827	9.3671	0.7995	9.8258	0.9964	0.6836	0.9864	0.7813
Touch down Pass	0.7572	9.9781	0.9771	1.4648	0.8481	7.9883	0.7572	11.5729	1.0000	0.1953	1.0000	0.0000
Tractor	0.8528	7.4414	0.8754	6.7383	0.8169	8.6328	0.7308	22.0325	0.9784	1.3672	0.9972	0.4883
Vidyo 1	0.9473	3.1250	0.9937	0.6707	0.9724	1.5625	0.9785	1.6602	1.0000	0.0977	1.0000	0.0000
Vidyo 3	0.8061	9.8633	1.0000	0.0000	0.9739	1.6602	0.9837	1.0742	1.0000	0.0000	1.0000	0.0000
Vidyo 4	0.9742	1.2695	0.9924	0.6836	0.9926	0.6736	0.9941	0.4759	0.9925	0.2930	1.0000	0.0000
Average	0.8344	7.1752	0.9640	2.0231	0.8775	5.8542	0.8583	8.0879	0.9895	0.6445	0.9919	0.4724

Table 7 NC and BER results for extracted watermarks after applying different lossy compression on watermarked videos (Part 2)

Videos	MPEG2		MXF		OGV		WEBM		WMV		XVID	
	NC	BER	NC	BER	NC	BER	NC	BER	NC	BER	NC	BER
Aspen	0.9953	0.2930	0.9980	0.0977	0.9757	1.2695	0.6985	17.0430	0.9973	0.2930	1.0000	0.0000
Blue sky	0.9916	0.5859	0.9980	0.0977	0.9924	0.4883	0.7633	12.2070	0.9925	0.6836	0.9875	1.0742
Control led Burn	0.9628	1.7578	0.9961	0.1953	0.9684	1.7578	0.7519	12.4023	0.9485	2.8320	0.9767	1.6602
Crowd run	0.8672	7.0313	0.9531	2.3438	0.7238	13.8672	0.7796	11.7188	0.9615	2.2461	0.9137	4.3945
Dinner	1.0000	0.0000	1.0000	0.0000	1.0000	0.0000	1.0000	0.0000	1.0000	0.0000	1.0000	0.0000
Factory	0.9237	3.8086	1.0000	0.0000	0.9676	1.7578	0.6884	16.1133	0.9848	0.9569	0.9758	1.4648
Four People	0.8645	6.5395	1.0000	0.0000	1.0000	0.0000	1.0000	0.0000	0.9377	3.5156	1.0000	0.0000
In to tree	0.8537	9.3574	0.9961	0.1953	0.9972	0.2930	0.7629	12.2070	0.9835	1.0742	0.9682	1.8555
Johnny	0.9276	5.6571	1.0000	0.0000	1.0000	0.0000	1.0000	0.0000	0.9648	1.9531	1.0000	0.0000
Kristen And Sara	0.8759	7.2783	1.0000	0.0000	1.0000	0.0000	0.9759	1.2695	0.9326	3.3203	1.0000	0.0000
Life	0.8369	8.5938	0.9570	2.1484	0.8542	6.3984	0.7869	10.8594	0.7768	9.9834	0.7964	9.3516
Mob cal ter	0.8178	9.5729	1.0000	0.0000	0.9942	0.5859	0.9576	2.6367	1.0000	0.0000	0.9862	0.7813
Old town cross	0.8225	9.8725	1.0000	0.0000	0.9974	0.5859	0.8823	5.9570	1.0000	0.0000	1.0000	0.0000
Park joy	0.7996	9.5438	0.9473	2.6367	0.6318	18.6523	0.6948	18.9023	0.8195	9.5703	0.8369	8.4570
Park run	0.8664	7.8248	1.0000	0.0000	1.0000	0.1953	0.8807	5.9570	1.0000	0.0000	0.9953	0.4883
Pedestrian area	0.9278	3.8086	0.9707	1.4648	0.6524	17.2852	0.7192	11.5482	0.9235	4.1016	0.8694	6.9336
Red Kayak	0.8737	6.3477	0.9941	0.2930	0.9482	3.0273	0.6931	18.7500	0.9617	2.2461	0.9865	1.1719
Riverbed	0.9448	2.9297	1.0000	0.0000	0.8267	9.0820	0.7764	11.6211	0.9775	1.3672	1.0000	0.0977
Rush Field Cuts	0.8167	9.4727	0.9980	0.0977	0.7775	19.3672	0.8347	8.5859	0.8357	8.3008	0.9273	4.1016
Rush hour	0.9954	0.4883	0.9922	0.3906	0.9437	3.2227	0.7381	6.8938	0.9861	1.1719	0.9972	0.3906
Shields ter	0.7854	9.6428	0.9980	0.0977	0.9871	1.1719	0.9549	2.6367	0.9952	0.3906	0.9938	0.6836
Speed Bag	1.0000	0.0000	1.0000	0.0000	1.0000	0.0000	0.9478	2.9297	0.9196	4.5898	1.0000	0.0000
Station 2	1.0000	0.1953	1.0000	0.0000	1.0000	0.0977	0.6872	15.8203	1.0000	0.0000	0.9943	0.5859

Table 7 (continued)

Videos	MPEG2		MXF		OGV		WEBM		WMV		XVID	
	NC	BER	NC	BER	NC	BER	NC	BER	NC	BER	NC	BER
Stockholm	0.8735	7.6715	1.0000	0.0000	1.0000	0.1953	0.9386	3.3203	0.9838	0.9749	0.9961	0.2930
Sunflower	0.8837	5.9570	1.0000	0.0000	0.8745	6.4453	0.7167	11.6721	0.9973	0.6836	0.8915	5.3711
Touch down Pass	0.9967	0.5859	1.0000	0.0000	0.9237	4.0039	0.8436	7.9102	0.9485	2.9297	0.9824	0.7813
Tractor	0.9678	2.0508	0.9902	0.4883	0.7622	12.0117	0.7056	12.8242	0.9876	1.1719	0.9682	1.9531
Vidyo 1	0.7549	15.3711	1.0000	0.0000	1.0000	0.0000	1.0000	0.0000	0.9238	3.8086	1.0000	0.0000
Vidyo 3	0.7695	14.6712	1.0000	0.0000	1.0000	0.0000	1.0000	0.0000	1.0000	0.0000	1.0000	0.0000
Vidyo 4	0.7581	15.4297	1.0000	0.0000	1.0000	0.0000	1.0000	0.0000	0.9755	1.5625	1.0000	0.0000
Average	0.8918	6.0780	0.9930	0.3516	0.9266	4.0587	0.8393	8.0595	0.9572	2.3243	0.9681	1.7297

where W is original watermark and EW is the extracted watermark from attacked video, respectively. In this equation m and n are the size of original watermark. Also bit error rate is defined by:

$$BER(W, EW) = \frac{\sum_{i=1}^{m}\sum_{j=1}^{n} W(i, j) \oplus EW(i, j)}{m \times n} \times 100 \tag{12}$$

where W is the original watermark and EW is the extracted watermark from attacked video. In this equation m and n are the size of original watermark. The NC and BER results between original watermark and extracted watermarks are shown in Tables 6 and 7. These results demonstrate that proposed video watermarking method highly resists against most lossy compression. In Fig. 7 it can be seen that for evaluating the proposed method, a variety of compression algorithms, including 18 different formats, are tested on 30 test videos.To

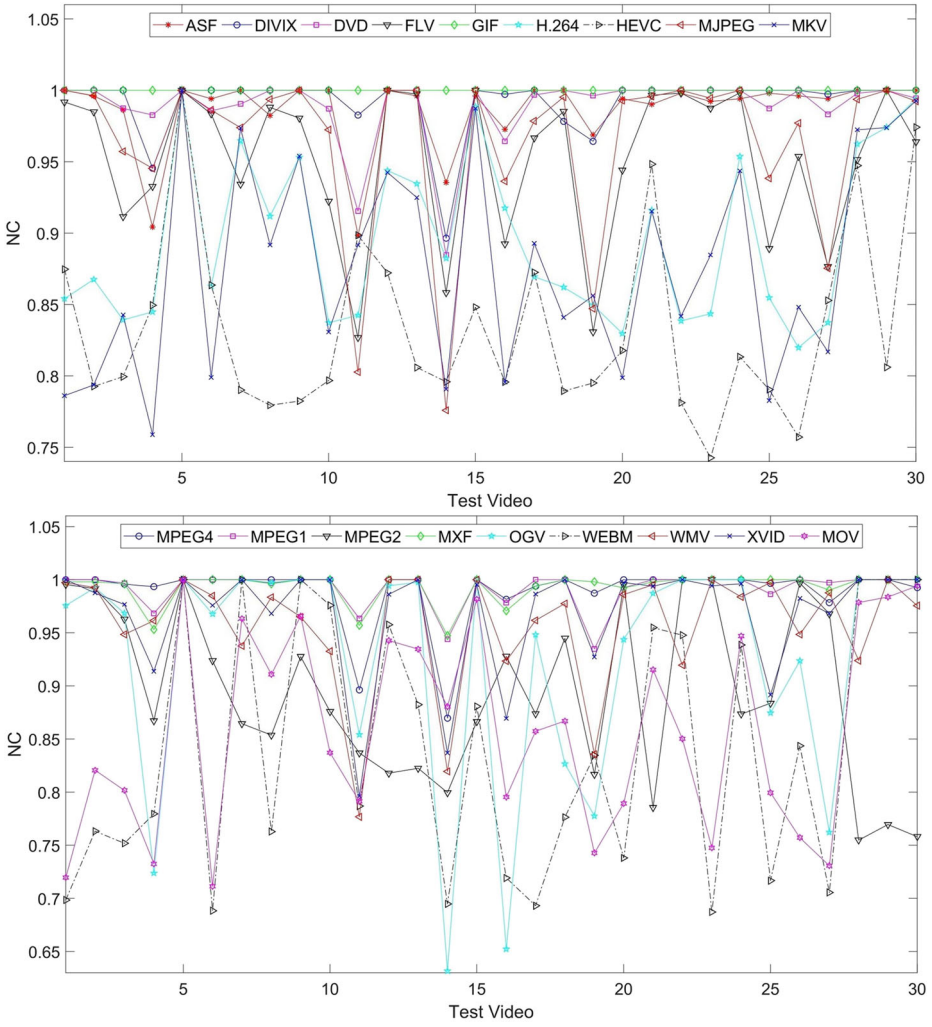

Fig. 7 Robustness analyze for test videos based on NC measure in compression attacks

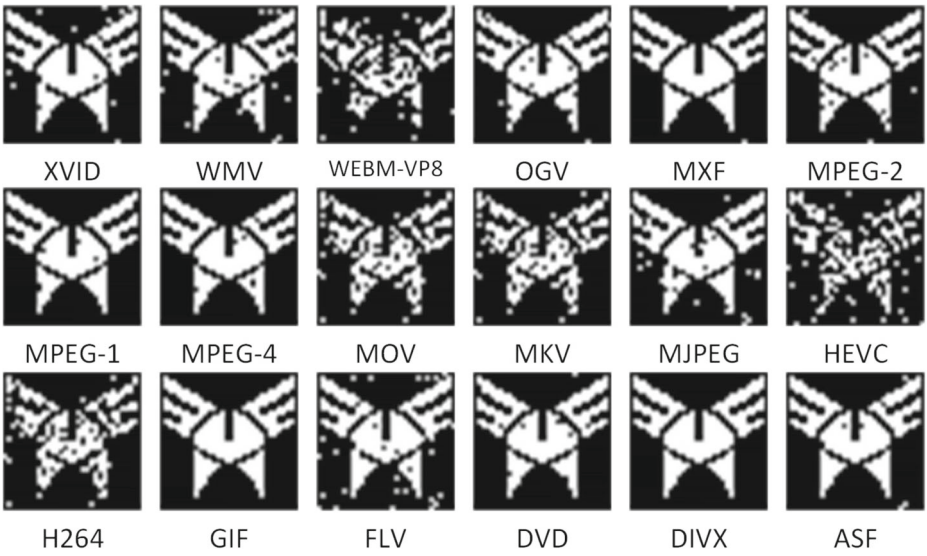

Fig. 8 Controlled Burn test video's extracted logo after various compression attacks

display and analyze the strength of the algorithm against different compression formats, the NC benchmark is calculated for all formats and is shown in this image. In terms of NC measure, it can be seen that the GIF format has the least damage to the watermarked video. Figure 8 displays extracted watermark after various compression attacks on Controlled burn test video. The proposed algorithm uses the threshold value (T) to balance the imperceptibility and robustness. In order to achieve the optimal state of the algorithm, different threshold values are evaluated. Figures 9 and 10 are illustrate the effect of the threshold T on the visual

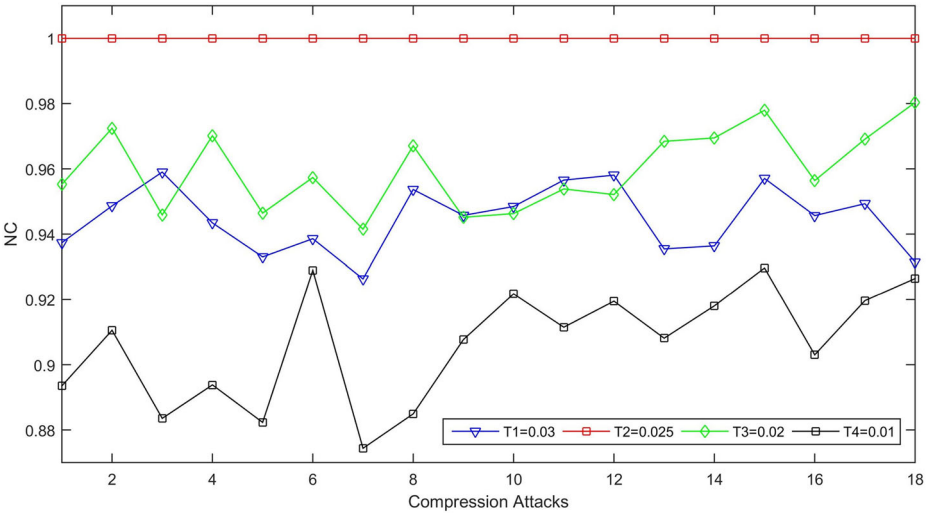

Fig. 9 Evaluation of various threshold value T effects on NC value on Dinner test image for compression attack

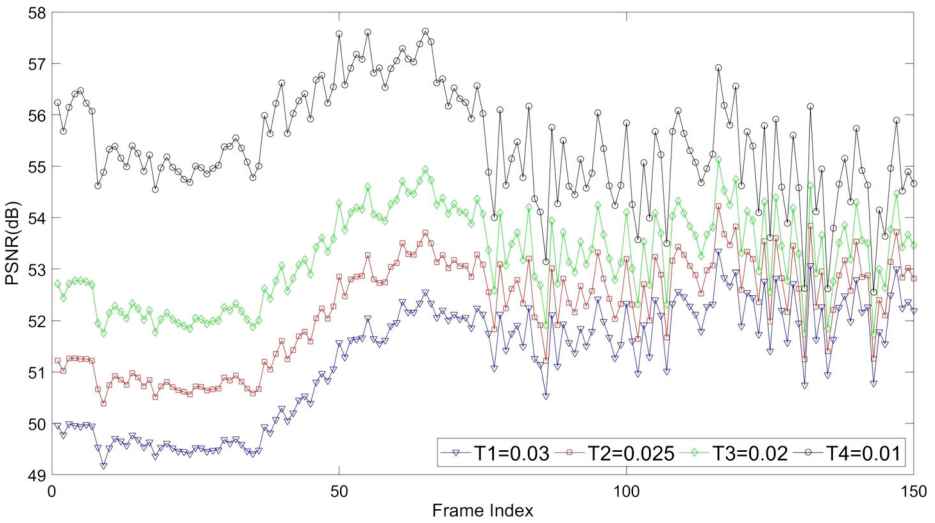

Fig. 10 Imperceptibility evaluation results based on $PSNR(dB)$ and for different threshold T on Dinner test video

quality(PSNR) of the embedding algorithm as well as the impact of compression on the videos. In Fig. 9, it can be seen that by setting the threshold $T = 0.01$, the correlation value, which is calculated based on the NC decreases and with decreasing the threshold T = 0.025t the NC increases and equals to one. The influence of the T parameter in Fig. 10 is also clear. In this figure with increasing the T parameter, the embedding visual quality increases and also with decrease threshold $T(0.025)$ the visual quality places around 50dB. In proposed algorithm in order to balance between embedding visual quality and high robustness against attacks the value of threshold set to be 0.025.

JPEG and JPEG2000 compressions are signal and image processing attacks. For digital video, this kind of attack is not a practical for evaluating the robustness of video watermarking algorithms, but several articles used them as attacks on watermarked videos. Therefore, this paper uses JPEG and JPEG2000 compression with different quality factors to evaluate the efficiency of the proposed algorithm. In Table 8, the values of BER and NC for JPEG compression attack with Quality Factors (QF) 10, 20, 30, 40 and 50, also JPEG2000 attack results with Compression Ratio (Ratio) 60, 70, 80 and 90 are displayed in Table 9.

5.3 Geometric attacks

The proposed method in this paper is a robust video watermarking technique specifically designed to resist against compression attacks. Generally, compression and format changing attacks on digital images and videos are very common in today's communication platform. Some of these attacks in their internal structure create geometric distortions in the multimedia file structure. One of the most common geometric attacks is scaling, which occurs in both GIF and H.264 formats.

A variety of geometric attacks including scaling with different sizes, cropping video frames at different rates and rotation attack with various angles are shown in Table 10 for

Table 8 NC and BER results for extracted watermarks after applying lossy JPEG on watermarked videos

Videos	QF= 10		QF= 20		QF= 30		QF= 40		QF= 50	
	NC	BER	NC	BER	NC	BER	NC	BER	NC	BER
Aspen	0.6797	16.0156	0.9004	4.9805	1.0000	0.0000	1.0000	0.0000	1.0000	0.0000
Blue sky	1.0000	0.0000	1.0000	0.0000	1.0000	0.0000	1.0000	0.0000	1.0000	0.0000
Control led Burn	1.0000	0.0000	1.0000	0.0000	1.0000	0.0000	1.0000	0.0000	1.0000	0.0000
Crowd run	1.0000	0.0000	1.0000	0.0000	1.0000	0.0000	1.0000	0.0000	1.0000	0.0000
Dinner	0.9980	0.0977	1.0000	0.0000	1.0000	0.0000	1.0000	0.0000	1.0000	0.0000
Factory	0.9707	1.4648	0.9941	0.2930	1.0000	0.0000	1.0000	0.0000	1.0000	0.0000
Four People	0.9785	1.0742	0.9941	0.2930	1.0000	0.0000	1.0000	0.0000	1.0000	0.0000
In to tree	1.0000	0.0000	1.0000	0.0000	1.0000	0.0000	1.0000	0.0000	1.0000	0.0000
Johnny	0.7012	14.9414	0.8086	9.5703	1.0000	0.0000	1.0000	0.0000	1.0000	0.0000
Kristen And Sara	0.6855	15.7227	0.6805	18.9227	0.9980	0.0977	1.0000	0.0000	1.0000	0.0000
Life	0.8809	5.9570	0.9844	0.7813	1.0000	0.0000	1.0000	0.0000	1.0000	0.0000
Mob cal ter	1.0000	0.0000	1.0000	0.0000	1.0000	0.0000	1.0000	0.0000	1.0000	0.0000
Old town cross	1.0000	0.0000	1.0000	0.0000	1.0000	0.0000	1.0000	0.0000	1.0000	0.0000
Park joy	0.9141	4.2969	0.9512	2.4414	1.0000	0.0000	1.0000	0.0000	1.0000	0.0000
Park run	1.0000	0.0000	1.0000	0.0000	1.0000	0.0000	1.0000	0.0000	1.0000	0.0000
Pedestrian area	0.7195	16.0234	0.8028	9.9609	1.0000	0.0000	1.0000	0.0000	1.0000	0.0000
Red Kayak	0.9980	0.0977	1.0000	0.0000	1.0000	0.0000	1.0000	0.0000	1.0000	0.0000
Riverbed	1.0000	0.0000	1.0000	0.0000	1.0000	0.0000	1.0000	0.0000	1.0000	0.0000
Rush Field Cuts	1.0000	0.0000	1.0000	0.0000	1.0000	0.0000	1.0000	0.0000	1.0000	0.0000
Rush hour	0.6751	17.8371	0.7141	16.8263	1.0000	0.0000	1.0000	0.0000	1.0000	0.0000
Shields ter	0.9980	0.0977	0.9980	0.0977	1.0000	0.0000	1.0000	0.0000	1.0000	0.0000
Speed Bag	0.9961	0.1953	1.0000	0.0000	1.0000	0.0000	1.0000	0.0000	1.0000	0.0000
Station 2	0.9766	1.1719	1.0000	0.0000	1.0000	0.0000	1.0000	0.0000	1.0000	0.0000

Table 8 (continued)

Videos	QF= 10		QF= 20		QF= 30		QF= 40		QF= 50	
	NC	BER	NC	BER	NC	BER	NC	BER	NC	BER
Stockholm	1.0000	0.0000	1.0000	0.0000	1.0000	0.0000	1.0000	0.0000	1.0000	0.0000
Sunflower	0.6762	18.8438	0.7283	15.7852	1.0000	0.0000	1.0000	0.0000	1.0000	0.0000
Touch down Pass	1.0000	0.0000	1.0000	0.0000	1.0000	0.0000	1.0000	0.0000	1.0000	0.0000
Tractor	1.0000	0.0000	1.0000	0.0000	1.0000	0.0000	1.0000	0.0000	1.0000	0.0000
Vidyo 1	0.9728	1.1719	1.0000	0.0000	1.0000	0.0000	1.0000	0.0000	1.0000	0.0000
Vidyo 3	0.9941	0.2930	1.0000	0.0000	1.0000	0.0000	1.0000	0.0000	1.0000	0.0000
Vidyo 4	1.0000	0.0000	1.0000	0.0000	1.0000	0.0000	1.0000	0.0000	1.0000	0.0000
Average	0.9272	3.8434	0.9519	2.6651	0.9999	0.0033	1.0000	0.0000	1.0000	0.0000

Table 9 NC and BER results for extracted watermarks after applying JPEG 2000 on watermarked videos

Videos	Ratio= 60		Ratio= 70		Ratio= 80		Ratio= 90	
	NC	BER	NC	BER	NC	BER	NC	BER
Aspen	1.0000	0.0000	1.0000	0.0000	1.0000	0.0000	0.9961	0.1953
Blue sky	1.0000	0.0000	0.7738	13.3086	0.7126	15.5716	0.6926	17.1682
Control led Burn	1.0000	0.0000	1.0000	0.0000	0.9941	0.2930	0.6983	15.1367
Crowd run	0.7106	14.9688	0.6995	15.3711	0.6718	17.3711	0.6571	18.5491
Dinner	1.0000	0.0000	1.0000	0.0000	1.0000	0.0000	1.0000	0.0000
Factory	1.0000	0.0000	0.9961	0.1953	0.9922	0.3906	0.8965	5.1758
Four People	1.0000	0.0000	0.9863	0.6836	0.7383	13.0859	0.6939	17.2843
In to tree	1.0000	0.0000	0.9316	3.4180	0.7012	14.9414	0.6815	18.3258
Johnny	0.9961	0.1953	0.9746	1.2695	0.9121	4.3945	0.8965	5.1758
Kristen And Sara	0.9512	2.4414	0.8848	5.7617	0.7041	16.7969	0.6724	19.1589
Life	0.9590	2.0508	0.7356	12.2188	0.7082	14.6275	0.6715	17.5862
Mob cal ter	0.9336	3.3203	0.9785	1.0742	0.9609	1.9531	0.9453	2.7344
Old town cross	0.9785	1.0742	0.7820	9.4023	0.7105	14.8319	0.6826	18.5872
Park joy	0.8824	7.4827	0.7739	9.7397	0.7268	13.8345	0.6788	17.3845
Park run	0.9863	0.6836	0.9785	1.0742	0.9609	1.9531	0.9453	2.7344
Pedestrian area	1.0000	0.0000	1.0000	0.0000	1.0000	0.0000	0.9883	0.5859
Red Kayak	1.0000	0.0000	0.9766	1.1719	0.9824	0.8789	0.9336	3.3203
Riverbed	1.0000	0.0000	1.0000	0.0000	1.0000	0.0000	1.0000	0.0000
Rush Field Cuts	0.9609	1.9531	0.9172	4.4883	0.8564	6.5437	0.7193	15.8607
Rush hour	1.0000	0.0000	1.0000	0.0000	1.0000	0.0000	1.0000	0.0000
Shields ter	0.8984	5.0781	0.9785	1.0742	0.9609	1.9531	0.9453	2.7344
Speed Bag	1.0000	0.0000	1.0000	0.0000	1.0000	0.0000	1.0000	0.0000
Station 2	1.0000	0.0000	1.0000	0.0000	1.0000	0.0000	1.0000	0.0000
Stockholm	0.9785	1.0742	0.8535	7.3242	0.9141	4.2969	0.8555	7.2746
Sunflower	1.0000	0.0000	1.0000	0.0000	1.0000	0.0000	0.9551	2.2461
Touch down Pass	1.0000	0.0000	1.0000	0.0000	1.0000	0.0000	0.9980	0.0682
Tractor	1.0000	0.0000	1.0000	0.0000	1.0000	0.0000	0.9707	1.4648
Vidyo 1	1.0000	0.0000	1.0000	0.0000	1.0000	0.0000	0.7871	10.6445
Vidyo 3	1.0000	0.0000	1.0000	0.0000	0.9980	0.0977	0.9863	0.6836
Vidyo 4	1.0000	0.0000	1.0000	0.0000	1.0000	0.0000	0.9961	0.1953
Average	0.9745	1.3441	0.9407	2.9192	0.9069	4.7938	0.8648	7.3425

displaying the performance and robustness of the proposed algorithm. Output results of this table are displayed based on the NC and BER(%) measures on Controlled Burn test video. According to the output results of this table, it can be clearly seen that, in addition to robustness against compression and format changing attacks, proposed method can resist against geometric attacks.

Table 10 NC and BER(%) results for extracted watermarks after applying geometric attacks such as scaling, rotation and cropping on watermarked Controlled Burn as sample video

	Resize				Cropping			Rotation				
Measures	Scale=2	Scale=0.9	Scale=0.5	Scale=0.3	15%	25%	50%	1^o	5^o	15^o	45^o	90^o
NC	0.9917	0.9939	0.9981	0.999	0.9947	0.8139	0.6318	0.9217	0.8925	0.8396	0.6218	0.4327
BER	1.32	1.01	0.73	0.32	2.58	12.78	17.52	3.72	10.55	14.93	21.37	37.52

Table 11 The comparison results of BER and NC between proposed method and some similar techniques after some attacks

Methods	No attacks		MPEG1		MPEG2		MPEG4		MJPEG	DIVX	XVID	H.264	
	PSNR	NC	BER	NC	BER	NC	BER	NC	NC	NC	NC	BER	NC
Proposed method	48.08	1	0.4724	0.9919	6.078	0.8918	0.6445	0.9895	0.9640	0.9926	0.961	5.9210	0.8950
Himeur [23]	46.90	×	×	×	×	×	×	×	1	×	×	×	0.9970
Preda [46]	47.84	×	×	×	27.73	×	×	×	×	×	×	×	×
Masoumi [41]	35.00	0.9450	×	×	×	0.96	×	×	×	×	×	×	0.9932
Xu [62]	39.65	0.9437	×	×	×	×	0.0537	0.90	×	×	×	×	×
M. ElArbi [15]	×	×	×	0.66	×	0.94	×	0.79	1	0.96	0.74	×	×
A. Tiwari [55]	42.25	0.9939	×	×	×	×	×	×	×	×	×	×	×
F. Alenizi [2]	45.35	0.8500	×	×	×	×	×	×	×	×	×	×	×
A. Q. M. Sabri [47]	48.87	1	×	×	×	×	×	×	×	×	×	×	×
I. Bayoudh [9]	×	×	×	×	×	×	0.1200	×	×	×	×	0.00	×
N. I. Yassin [65]	45.41	0.7520	0.5371	×	×	×	×	×	×	×	×	×	×
A. Bhardwaj [10]	×	×	×	×	0.2013	×	×	×	×	×	×	0.06	×
C. Wu [59]	40.46	0.7032	×	×	×	×	×	×	×	×	×	×	×
P.-C. Su [52]	45.02	×	×	×	×	0.00	×	×	×	×	×	0.00	×
J. Xuemei [63]	46.69	×	×	×	×	0.86	×	0.89	×	×	×	×	0.8500
Rank	2	1	1	1	2	3	3	1	3	1	1	4	3

(×) There is no result reported

Table 12 The Robustness evaluation based on NC measure between proposed method and some similar techniques after lossy JPEG

Methods	QF= 30	QF= 50	QF= 60	QF= 70	QF= 80	QF= 90
Proposed method	0.9999	1.0000	1.0000	1.0000	1.0000	1.0000
Bhardwaj et al. [10]	×	0.9805	1.0000	1.0000	0.9980	1
Singh [50]	×	0.5058	×	0.5595	0.6396	0.9960
Chen [13]	0.8371	×	×	×	×	×
Yassin [65]	0.5382	0.6465	×	×	0.7324	×
Chen [11]	0.9877	×	×	×	×	×
Rank	1	1	1	1	1	1

(×) There is no result reported

6 Comparison with similar methods

This section compares proposed method with some similar video watermarking techniques in the compression field. This comparison is done in terms of PSNR and NC values after compressing watermarked videos. In order to investigate the robustness of proposed method, Table 11 shows the NC and BER results between original watermark and extracted watermark in different lossy compression (like MPEG2, MPEG4, MJPEG, etc) and compares with the results of other methods. Table 12 demonstrates the comparison results of NC between proposed method and similar methods after lossy JPEG compression with different quality factors. The analysis results and comparison with other existing methods illustrate that the proposed technique resists against different types of lossy video compression and outperforms in the case of protecting watermark. Additionally, the chaotic embedding and correction process of the proposed algorithm guarantee more security and provide a good method to protect videos copyright.

7 Conclusion and future work

Watermarking is one of the common methods to protect digital media such as video. In proposed method, the watermark is embedded into the video robustly. This article proposes a blind method and performs the processes of embedding and extraction in the contourlet transform domain.

In order to increase the robustness of the proposed watermarking algorithm and using the orthogonal property, SVD utilized in the proposed algorithm. Proposed approach is a free-format video watermarking algorithm, a new chaotic map based on Newton complex model is used. This paper focuses specifically on compression attacks on HD videos. Widespread use of videos in communication and commercial industries are the main reasons to propose this work. According to the obtained results, it can be concluded that the proposed algorithm has good values for the PSNR and SSIM measures and provides acceptable imperceptibility after embedding watermark. Therefore, Robustness analysis based on BER and NC displays that the proposed method is highly robust against most video compression attacks. By observing Tables 6 and 7, it can be seen that the proposed technique does not have enough robustness against HEVC and H.264 compression formats, and the

BER for these two formats are high. For future work, we will try to resolve the above mentioned problem and increase the robustness of proposed method against HEVC and H.264 formats.

Compliance with Ethical Standards

Conflict of interests All authors declare that they have no conflict of interest.

References

1. Agilandeeswari L, Ganesan K (2016) A robust color video watermarking scheme based on hybrid embedding techniques. Multimed Tools Appl 75(14):8745–8780
2. Alenizi F, Kurdahi F, Eltawil A, Aljumah A (2015) Dwt-based watermarking technique for video authentication. In: 2015 IEEE international conference on electronics, circuits, and systems (ICECS). IEEE, pp 41–44
3. Ansari IA, Pant M (2017) Multipurpose image watermarking in the domain of dwt based on svd and abc. Pattern Recogn Lett 94:228–236
4. Arora SM et al (2018) A dwt-svd based robust digital watermarking for digital images. Procedia Comput Sci 132:1441–1448
5. Asikuzzaman M, Alam MJ, Lambert AJ, Pickering MR (2012) A blind digital video watermarking scheme with enhanced robustness to geometric distortion. In: 2012 International conference on digital image computing techniques and applications (DICTA). IEEE, pp 1–8
6. Bahrami Z, Tab FA (2018) A new robust video watermarking algorithm based on surf features and block classification. Multimed Tools Appl 77(1):327–345
7. Barani MJ, Ayubi P, Jalili F, Valandar MY, Azariyun E (2015) Image forgery detection in contourlet transform domain based on new chaotic cellular automata. Secur Commun Netw 8(18):4343–4361
8. Barani MJ, Valandar MY, Ayubi P (2015) A secure watermark embedding approach based on chaotic map for image tamper detection. In: 2015 7th conference on information and knowledge technology (IKT). IEEE, pp 1–5
9. Bayoudh I, Jabra SB, Zagrouba E (2017) Online multi-sprites based video watermarking robust to collusion and transcoding attacks for emerging applications. Multimed Tools Appl: 1–19
10. Bhardwaj A, Verma VS, Jha RK (2017) Robust video watermarking using significant frame selection based on coefficient difference of lifting wavelet transform. Multimed Tools Appl: 1–20
11. Chen L, Zhao J (2015) Adaptive digital watermarking using rdwt and svd. In: 2015 IEEE international symposium on haptic, audio and visual environments and games (HAVE). IEEE, pp 1–5
12. Chen L, Zhao J (2017) Robust contourlet-based blind watermarking for depth-image-based rendering 3d images. Signal Process Image Commun 54:56–65
13. Chen L, Zhao J (2018) Contourlet-based image and video watermarking robust to geometric attacks and compressions. Multimed Tools Appl 77(6):7187–7204
14. Cox I, Miller M, Bloom J, Fridrich J, Kalker T (2007) Digital watermarking and steganography. Morgan Kaufmann, San Mateo
15. El'Arbi M, Koubaa M, Charfeddine M, Amar CB (2011) A dynamic video watermarking algorithm in fast motion areas in the wavelet domain. Multimed Tools Appl 55(3):579–600
16. Fan M, Wang H (2018) An enhanced fragile watermarking scheme to digital image protection and self-recovery. Signal Process Image Commun 66:19–29
17. Farri E, Ayubi P (2018) A blind and robust video watermarking based on iwt and new 3d generalized chaotic sine map. Nonlinear Dynamics: 1–23
18. Foundation X (2018) Xiph.org video test media [derf's collection]. https://media.xiph.org/video/derf/
19. Furht B (1998) Handbook of Internet and multimedia systems and applications, vol 6. CRC Press, Boca Raton
20. Gaj S, Rathore AK, Sur A, Bora PK (2017) A robust watermarking scheme against frame blending and projection attacks. Multimed Tools Appl 76(20):20755–20779
21. Goldberger AL (1996) Non-linear dynamics for clinicians: chaos theory, fractals, and complexity at the bedside. The Lancet 347(9011):1312–1314
22. Hasnaoui M, Mitrea M (2014) Multi-symbol qim video watermarking. Signal Process Image Commun 29(1):107–127

23. Himeur Y, Boukabou A (2017) A robust and secure key-frames based video watermarking system using chaotic encryption. Multimed Tools Appl: 1–25
24. Huang H-Y, Yang C-H, Hsu W-H (2010) A video watermarking technique based on pseudo-3-d dct and quantization index modulation. IEEE Trans Inform Forensics Secur 5(4):625–637
25. Hubbard J, Schleicher D, Sutherland S (2001) How to find all roots of complex polynomials by Newton's method. Inventiones Mathematicae 146(1):1–33
26. Jacquin AE (1992) Image coding based on a fractal theory of iterated contractive image transformations. IEEE Trans Image Process 1(1):18–30
27. Jiang Y-G, Wu Z, Wang J, Xue X, Chang S-F (2018) Exploiting feature and class relationships in video categorization with regularized deep neural networks. IEEE Transactions on Pattern Analysis and Machine Intelligence 40(2):352–364. https://doi.org/10.1109/TPAMI.2017.2670560
28. Karmakar A, Phadikar A, Phadikar BS, Maity GK (2016) A blind video watermarking scheme resistant to rotation and collusion attacks. Journal of King Saud University-Computer and Information Sciences 28(2):199–210
29. Klema V, Laub A (1980) The singular value decomposition: its computation and some applications. IEEE Trans Automatic Control 25(2):164–176
30. Kuehne H, Jhuang H, Garrote E, Poggio T, Serre T (2011) HMDB: a large video database for human motion recognition. In: Proceedings of the international conference on computer vision (ICCV)
31. Lian S (2008) Multimedia content encryption: techniques and applications, Auerbach Publications
32. Lin SD, Chen C-F (2000) A robust dct-based watermarking for copyright protection. IEEE Trans Consum Electron 46(3):415–421
33. Liu H, Xiao D, Zhang R, Zhang Y, Bai S (2016) Robust and hierarchical watermarking of encrypted images based on compressive sensing. Signal Process Image Commun 45:41–51
34. Liu X, Zhao R, Li F, Liao S, Ding Y, Zou B (2017) Novel robust zero-watermarking scheme for digital rights management of 3d videos. Signal Process Image Commun 54:140–151
35. Liu Y, Zhao J (2010) A new video watermarking algorithm based on 1d dft and radon transform. Signal Process 90(2):626–639
36. Lu Z-M, Xu D-G, Sun S-H (2005) Multipurpose image watermarking algorithm based on multistage vector quantization. IEEE Trans Image Process 14(6):822–831
37. Madine F, Akhaee MA, Zarmehi N (2018) A multiplicative video watermarking robust to h. 264/Avc compression standard. Signal Process Image Commun 68:229–240
38. Mandelbrot BB (1982) The fractal geometry of nature, vol 1. WH Freeman, New York
39. Mansouri A, Aznaveh AM, Torkamani-Azar F, Kurugollu F (2010) A low complexity video watermarking in h. 264 compressed domain. IEEE Trans Inform Forensics Secur 5(4):649–657
40. Marszałek M, Laptev I, Schmid C (2009) Actions in context. In: IEEE conference on computer vision & pattern recognition
41. Masoumi M, Amiri S (2013) A blind scene-based watermarking for video copyright protection. AEU-International Journal of Electronics and Communications 67(6):528–535
42. Najafi E, Loukhaoukha K (2019) Hybrid secure and robust image watermarking scheme based on svd and sharp frequency localized contourlet transform. Journal of Information Security and Applications 44:144–156
43. Ni Z, Shi Y-Q, Ansari N, Su W (2006) Reversible data hiding. IEEE Trans Circuits Syst Video Technol 16(3):354–362
44. O'Keeffe GS, Clarke-Pearson K et al (2011) The impact of social media on children, adolescents, and families. Pediatrics 127(4):800–804
45. Podilchuk CI, Delp EJ (2001) Digital watermarking: algorithms and applications. IEEE Signal Process Magazine 18(4):33–46
46. Preda RO, Vizireanu DN (2010) A robust digital watermarking scheme for video copyright protection in the wavelet domain. Measurement 43(10):1720–1726
47. Sabri AQM, Mansoor AM, Obaidellah UH, Faizal ERM et al (2017) Metadata hiding for uav video based on digital watermarking in dwt transform. Multimed Tools Appl 76(15):16239–16261
48. Seitz J (2005) Digital watermarking for digital media, IGI Global
49. Shao Z, Shang Y, Zeng R, Shu H, Coatrieux G, Wu J (2016) Robust watermarking scheme for color image based on quaternion-type moment invariants and visual cryptography. Signal Process Image Commun 48:12–21
50. Singh KM (2017) A robust rotation resilient video watermarking scheme based on the sift. Multimed Tools Appl: 1–26
51. Song H, Yu S, Yang X, Song L, Wang C (2008) Contourlet-based image adaptive watermarking. Signal Process Image Commun 23(3):162–178

52. Su P-C, Kuo T-Y, Li M-H (2017) A practical design of digital watermarking for video streaming services. J Vis Commun Image Represent 42:161–172
53. Tekalp AM (2015) Digital video processing. Prentice Hall Press, Englewood Cliffs
54. Thind DK, Jindal S (2015) A semi blind dwt-svd video watermarking. Procedia Comput Sci 46:1661–1667
55. Tiwari A, Ojha SK, Pantiukhin D (2017) An effective approach for secure video watermarking based on h. 264 coding standard. In: 2017 3rd international conference on computational intelligence & communication technology (CICT). IEEE, pp 1–5
56. Valandar MY, Ayubi P, Barani MJ (2017) A new transform domain steganography based on modified logistic chaotic map for color images. J Inform Secur Appl 34:142–151
57. Valandar MY, Barani MJ, Ayubi P, Aghazadeh M (2018) An integer wavelet transform image steganography method based on 3d sine chaotic map. Multimed Tools Appl: 1–19
58. Wang Y, Doherty JF, Van Dyck RE (2002) A wavelet-based watermarking algorithm for ownership verification of digital images. IEEE Trans Image Process 11(2):77–88
59. Wu C, Zheng Y, Ip W, Chan C, Yung K, Lu Z (2011) A flexible h. 264/Avc compressed video watermarking scheme using particle swarm optimization based dither modulation. AEU-International Journal of Electronics and Communications 65(1):27–36
60. Wu D, Kong W, Yang B, Niu X (2009) A fast svd based video watermarking algorithm compatible with mpeg2 standard. Soft Comput 13(4):375–382
61. Xu D, Wang R, Wang J (2011) A novel watermarking scheme for h. 264/avc video authentication. Signal Process Image Commun 26(6):267–279
62. Xu D-W (2007) A blind video watermarking algorithm based on 3d wavelet transform. In: 2007 international conference on computational intelligence and security. IEEE, pp 945–949
63. Xuemei J, Quan L, Qiaoyan W (2013) A new video watermarking algorithm based on shot segmentation and block classification. Multimed Tools Appl 62(3):545–560
64. Yadav J, Sehra K (2018) Large scale dual tree complex wavelet transform based robust features in pca and svd subspace for digital image watermarking. Procedia Comput Sci 132:863–872
65. Yassin NI, Salem NM, El Adawy MI (2014) Qim blind video watermarking scheme based on wavelet transform and principal component analysis. Alexandria Engineering Journal 53(4):833–842